



# Geometry design and performance evaluation of thermoelectric generator

R. S. Kondaguli and P. V. Malaji<sup>a</sup>

Energy Harvesting and IoT Lab, B.L.D.E A's V.P Dr. P G Halakatti College of Engineering and Technology (Affiliated to Visvesvaraya Technological University), Vijayapur, Karnataka 586103, India

Received 25 September 2021 / Accepted 20 February 2022

© The Author(s), under exclusive licence to EDP Sciences, Springer-Verlag GmbH Germany, part of Springer Nature 2022

**Abstract** A thermoelectric generator is a solid-state device that directly converts heat into electricity without any moving parts. The problem with these devices is that they are less efficient. The present study considers modeling and numerical simulation of a thermoelectric generator of different shapes to evaluate their efficacy. Effective material properties of TEG are used in CPM model of analysis. Different shapes of the leg have been simulated, keeping the same isothermal boundary conditions. The effect of the cross-section area of the leg and leg length. Hot-side and cold-side junction temperature and thermal stress developed are reported. Results shows that trapezoid generators are better from efficiency point of view where as square and circular cross-section leg produces more power.

## List of symbols

$z_t$	Material figure of merit
$ZT$	Device figure of merit
$\alpha$	Seebeck coefficient
$\kappa$	Thermal conductivity
$\rho$	Resistivity of material
$L$	Length of leg
$A$	Cross-section area
$Q_{out}$	Heat flow rate out from cold junction
$Q_{in}$	Heat flow rate into hot junction
$R$	Total resistance
$R_{in}$	Internal resistance
$R_L$	Load resistance
$T_h$	Hot junction temperature
$T_c$	Cold junction temperature
$P_{out}$	Power output from thermoelectric generator
$\eta_{th}$	Thermal efficiency

## 1 Introduction

Energy has always been among the essential resources that endorses human society's progress, evolution, and prosperity. It is expected that by 2030, world will be connected by trillions of sensors. It is not accessible to power all these sensors in remote places. Energy harvesting is a viable solution. It can be of several ways like vibration energy harvesting [1,2], thermal energy har-

vesting [3,4], etc. Thermal energy is one of most sought energy sources which can be utilized to power the sensors at isolated locations. Thermal energy is low-grade energy; during different applications, there is a loss of 66% of thermal energy as waste heat. At high temperatures (500 °C to 1000 °C), thermal energy is converted to mechanical energy very efficiently. At medium and low temperatures (150–500 °C and 80–150 °C), energy conversion is difficult. This low-temperature thermal energy can be converted to electrical energy using thermoelectric devices. Recovery of even a tiny fraction of this waste heat and conversion to electrical energy will significantly impact the industry and society [5–7]. A thermoelectric generator directly converts thermal energy to electrical energy. The thermoelectric generator is used in various applications such as waste heat recovery, satellites, power generation, etc. Hence, a more significant number of industries are producing thermoelectric generators. The efficiency of thermoelectric generator varies from [8] 8.9 to 12% [9]. Practically, it is still lower. A thermoelectric generator is a solid-state device consisting of semiconductors connected by metal plates and sandwiched between ceramic substrates. The emf is generated when two sides of the thermoelectric generator are at different temperatures [10,11].

A thermoelectric material should have high seebeck coefficient low electrical resistivity and thermal conductivity. The above three terms can be combined in one term  $z = \frac{\alpha^2}{\rho\kappa} \cdot z$  is having a unit of  $K^{-1}$ ; it is usually expressed by a non-dimensional term called  $z_t$  called material figure of merit; the higher the  $z_t$  value, the better is the thermoelectric material. Thermal conduc-

<sup>a</sup>e-mail: [pradeepmalaji@bldeacet.ac.in](mailto:pradeepmalaji@bldeacet.ac.in) (corresponding author)

tivity has two parts: the electronic part and lattice part, and the thermal conductivity of the lattice part can be reduced [12]. With nanotechnology, nowadays, high zt materials are produced [10]. SnSe thermoelectric material of zt 2.6 [13] of p-type and zt of 2.8 [14] for n-type material have been reported.

During fabrication of thermoelectric devices from material, the efficiency will reduce. Device figure of merit is given as ZT as in Eq. 1. Thermoelectric devices can work as effectively as present mechanical devices if device ZT is of 4 [15]. Thermoelectric power generation is a promising technology for future power generation and waste heat recovery. The problem with TEG is that they are less efficient. The efficiency of TEG reaches Carnot efficiency as figure of merit (ZT) tends to infinity. Presently, most of the commercial thermoelectric devices are made of  $\text{Bi}_2\text{Te}_3$ . ZT of the commercially available thermoelectric device is about 1

$$\text{ZT} = \frac{(\alpha_p - \alpha_n)^2}{[(k_p \rho_n)^{\frac{1}{2}} + (k_n \rho_p)^{\frac{1}{2}}]^2} T. \quad (1)$$

Characterization of thermoelectric generators involves measuring electrical, thermal, and thermoelectric properties. Performance evaluation of thermoelectric generators done previously shows considerable deviation in the results from one lab to other [16]. Properties of thermoelectric materials are temperature-dependent. We can use constant material properties called effective material properties for simulation purpose. Effective material properties of TEG are not calculated directly by experiments. These are calculated theoretically; it includes the effect of resistance of legs, metal electrodes resistance, ceramic plate resistance, and contact resistances. These properties can be utilized for TEG simulation [17]. Thermoelectric generators simulated with effective material properties will give excellent results [18] and results are comparable with experimental results. Most of the manufacturers do not provide material properties [19]. The manufacturer provides maximum parameters; from these by a reverse method, we can calculate effective material properties. The module properties calculated from manufacturers data by maximum parameters are reported by Simon Lineykin [20].

The thermoelectric generator's performance depends not only on the material property but also on that geometric shape. Based on the application TEG can be of different shapes like annular, flat. The dimensions of the leg play a predominant role on performance of thermoelectric generator. By varying the length of the leg, the performance of TEG can be improved [12, 21]. Rowe in 1992 [22] reported that by decreasing the length of leg by 55% increases power by 48% and efficiency decreases by 10%. Sumeet [23] studied automotive exhaust thermoelectric generator and reported that efficacy of TEG depends mainly on on current, junction temperature difference, leg length, and ratio of cross section area of P- and N-type leg  $\frac{A_p}{A_n}$ . A dimensionless parameter called shape parameter is defined which signifies the

variation of cross section along the length of TEG [24]. As shape parameter increases power decreases, but efficiency increases. Fan et al. [25] presented mathematical and numerical simulation; they found that for constant heat flux, efficiency decreases as cross-section area increases. He et al. [26] carried performance evaluation of TEG and found that performance increases with increase in temperature difference, but decreases with increase in cross-section area. Fabián-Mijangos et al. [27] fabricated asymmetric TEG and also performed numerical simulation. It shows that asymmetric leg is having potential to improve efficiency and power. Literature shows that there is scope to improve the geometry of the thermoelectric leg to improve power and efficiency.

The performance of thermoelectric generator depends on the heat absorbed at hot junction, rejected at cold junction and load resistance. A thermoelectric generator produces more power when the load resistance is equal to internal resistance. Load resistance is constant for a given application. The internal resistance can be changed by varying the length, cross-section area, and other geometric parameters of the leg. Recent days, there is tremendous improvement in zt of thermoelectric materials. However, only Bismuth telluride TE modules are commercially available. Mechanical strength is significant in production of bulk TEG. The present work focuses on performance evaluation of a commercial thermoelectric generator by simulating. Comparison of these results with the experimental results reported Lee et al. [28] and data sheet provided by the manufacture [29] and analytical results [30] are presented in Sect. 3. Effect of geometric shapes on power output and efficiency for uni-couple thermoelectric generator is presented in Sect. 4. Thermal stress developed are also evaluated and compared for different shape of legs.

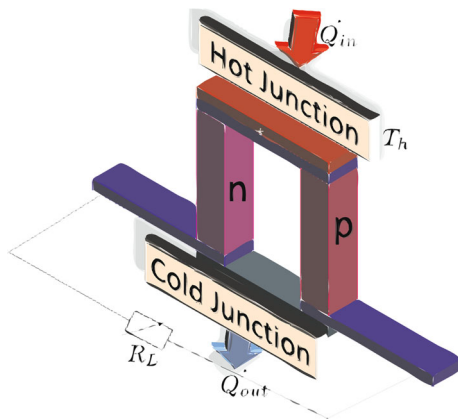
## 2 Methodology

Figure 1 shows an uni-couple thermoelectric generator. P-type and N-type semiconductors are connected electrically in series. Thermally in parallel, connected by a metal electrode, sandwiched between the ceramic substrate.

In this section, mathematical modeling and finite-element method of simulation is explained. The simulation is done using commercial software ANSYS [31]. Effective material properties are used for simulation. The method to analyze TEG and how to find the effective material properties are as follows.

### 2.1 Performance evaluation of thermoelectric generator by constant properties method

Lofee [32] was the first to propose constant property method [CPM] approximation. The properties of the thermoelectric module are temperature-dependent;



**Fig. 1** Uni-couple Thermoelectric Generator

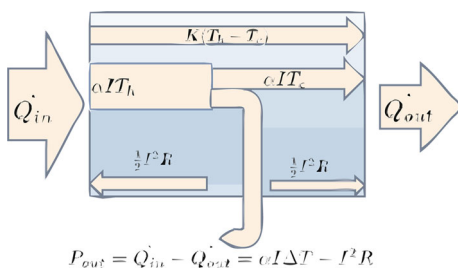


**Fig. 2** Different heat contributions in TEG

averaging the properties was practically proposed by Lofee. CPM model uses constant Thermoelectric properties. Ponnusamy et al. [33] reported the discrepancy of CPM model. CPM approximation formulae are listed below. In the present work, constant effective material properties are used in CPM model. Let us consider a thermoelectric material; one side is maintained at temperature higher temperature  $T_h$ . Another side is at a temperature  $T_c$ . As shown in Fig. 2, thermodynamic analysis is as follows. Thermal power input to the element

$$\dot{Q}_{in} = \alpha T_h I - \frac{1}{2} I^2 R + \kappa(T_h - T_c). \quad (2)$$

Thermal power output from the element

$$\dot{Q}_{out} = \alpha T_c I + \frac{1}{2} I^2 R + \kappa(T_h - T_c). \quad (3)$$

**Table 1** Effective properties of TEG material [28]

Material	Thermal conductivity (w/mk)	Seebeck coefficient (mV/k)	Electrical resistivity (Ohm.cm)	Youngs modulus (Gpa)	Poisson ratio	CTE (/K)	Specific heat (j/kgk)
N-Type	1.62	-0.167	0.00153	45	0.22	$1.6 * 10^{-5}$	154
P-Type	1.62	0.167	0.00153	45	0.22	$1.6 * 10^{-5}$	154
Copper	386						
Resistor			Varies				

Power produced by TEG element can be calculated as

$$P_{out} = \dot{Q}_{in} - \dot{Q}_{out} = \alpha I \Delta T - I^2 R. \quad (4)$$

Usually, thermoelectric devices are made up of P- and N-Type semiconductors. As shown if Fig. 1 for this case, current is calculated as

$$I = \alpha \frac{T_h - T_c}{R_L + R_i}, \quad (5)$$

where  $R_L$  is load resistance and  $R_i$  is internal resistance. Internal resistance is the summation of resistance of P-Type, N-Type semiconductors and contact resistances. P-Type resistance is calculated as  $R_p = \frac{\rho_p L}{A}$ ; N-Type resistance is calculated as  $R_n = \frac{\rho_n L}{A}$ . Total Seebeck coefficient of uni-couple is  $\alpha$  is  $\alpha = \alpha_p - \alpha_n$ ; where  $\alpha_p$  &  $\alpha_n$  are absolute Seebeck coefficients.

If n is number of P-N pairs, voltage is calculated as

$$V = n \alpha \left( \frac{R_L}{R_i} \right) \left( \frac{T_h - T_c}{\frac{R_L}{R_i} + 1} \right). \quad (6)$$

Efficiency is be calculated as

$$\eta_{th} = \frac{P_{out}}{\dot{Q}_{in}}. \quad (7)$$

Equation 4 is used to calculate power and Eq. 7 to calculate efficiency. Effective material properties used are listed in Table 1 [28].

### 2.2 Simulation of thermoelectric generator

The present work is to simulate thermoelectric generator using commercial software, which uses FEM calculations. Finite-element method was first proposed by Courant [34]. FEA method was first used to simulate thermoelectricity in 1996 by Lau et al. [35]. This method is useful, because it can handle temperature-dependent thermoelectric properties. Different types of boundary conditions and loads can be applied. Arbitrary shapes can be analyzed effectively. Commercial softwares with graphical interface having FEM algorithm are available now. ANSYS Thermal Electric uses coupled thermal electric equations using FEM method. It is suitable for thermoelectric analysis. The study

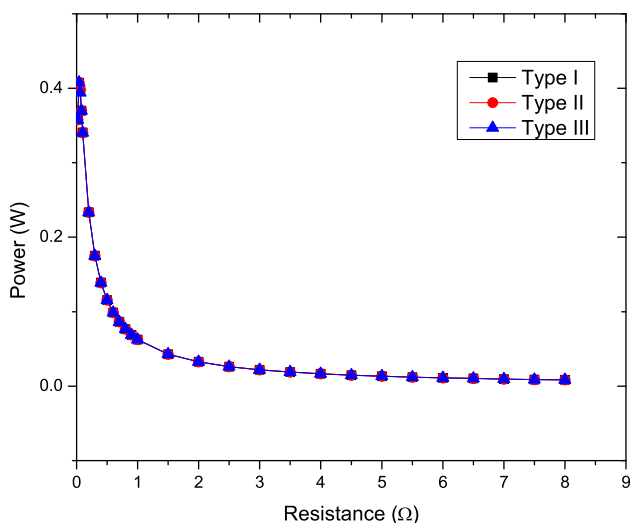
**Table 2** Grid Details

Particulars	Meshing Type-I	Meshing Type-II	Meshing Type-III
Nodes	3909	18,879	20,000
Elements	500	3296	2500

includes simulation of commercially available HiZ-2 thermoelectric module. Modeling is done in Design Modeler. Mesh is generated in ANSYS meshing tool. This model has 97 P-N pair, as shown in Fig. 5a. For optimization purposes, the shape of the leg is changed to circular, as shown in Fig. 5b. Figure 4 shows a model of different shapes of uni-couple thermoelectric generator. A commercially available thermoelectric module is square in shape. In this work, circular, trapezoid, and cone-shaped legs are considered for analysis for the uni-couple thermoelectric module. For uni-couple analysis, cross-section area of leg of square and circular are kept constant. A new design, as shown in Fig. 4f square with hole, has been proposed. Performance and thermal stress analysis has been done for different shapes of TEG.

### 2.3 Grid independence test

The grid independence test is done on uni-couple TEG. The analysis is done for different grid sizes keeping boundary conditions constant, as shown in Fig. 3. The square leg semiconductors have been used with the hot junction temperature of 700 °C and cold junction temperature of 30 °C. Convergence is attained at 500 elements.

**Fig. 3** Grid independence test

## 3 Performance analysis of 97 P–N pair thermoelectric generator

A 97 P–N pair thermoelectric module is simulated using effective material properties. The temperature profile of a square thermoelectric module is simulated with dimensions of commercially available HiZ-2 thermoelectric module, as shown in Fig. 8a. Temperature distribution of circular pillar TEG potential variant of square TEG is shown in Fig. 8b. Using the effective material properties as proposed by HoSung Lee [28], HiZ-2 Thermoelectric module is analysed with temperatures  $T_h = 230\text{ °C}$  and  $T_c = 30\text{ °C}$ . Simulation results are obtained from ANSYS, analytical results are obtained from Eq. 4, and experimental results are taken from Lee et al. [28]. From Fig. 6, it is observed that the simulated and analytical results are in well agreement with experimental results as reported HoSung Lee et al. [28]. The variation of power with current at optimal load resistance is shown in Fig. 7a, which is parabolic in nature. The variation of voltage with current is linear (Fig. 7b).

To understand effect of shape on the performance of TEG, the legs with square and circular cross sections are presented in Fig. 9. Isothermal hot junction temperature  $T_h = 250\text{ °C}$  and cold junction temperature as  $T_c = 50\text{ °C}$ , Hi-Z2 Thermoelectric module is simulated. Variation of power with load is plotted as in Fig. 9.

Figure 9 shows comparison of power for square and circular leg thermoelectric generator and data sheet of manufacturer of HiZ-2 [29]. Cross-section area is not identical for square and circular leg. Cross-section area of square leg is  $2.102\text{ mm}^2$  and that of circular is  $1.65\text{ mm}^2$ . Length of both legs is 2.87 mm. The cross-section area of square leg is more; hence, its internal resistance is low. It is observed that square leg TEG is better at lower load resistance and circular leg TEG has higher output at higher load resistance due to the difference in internal TEG resistance introduced by shape change. Based on the external load, TEG can be designed as square or circular to get more power.

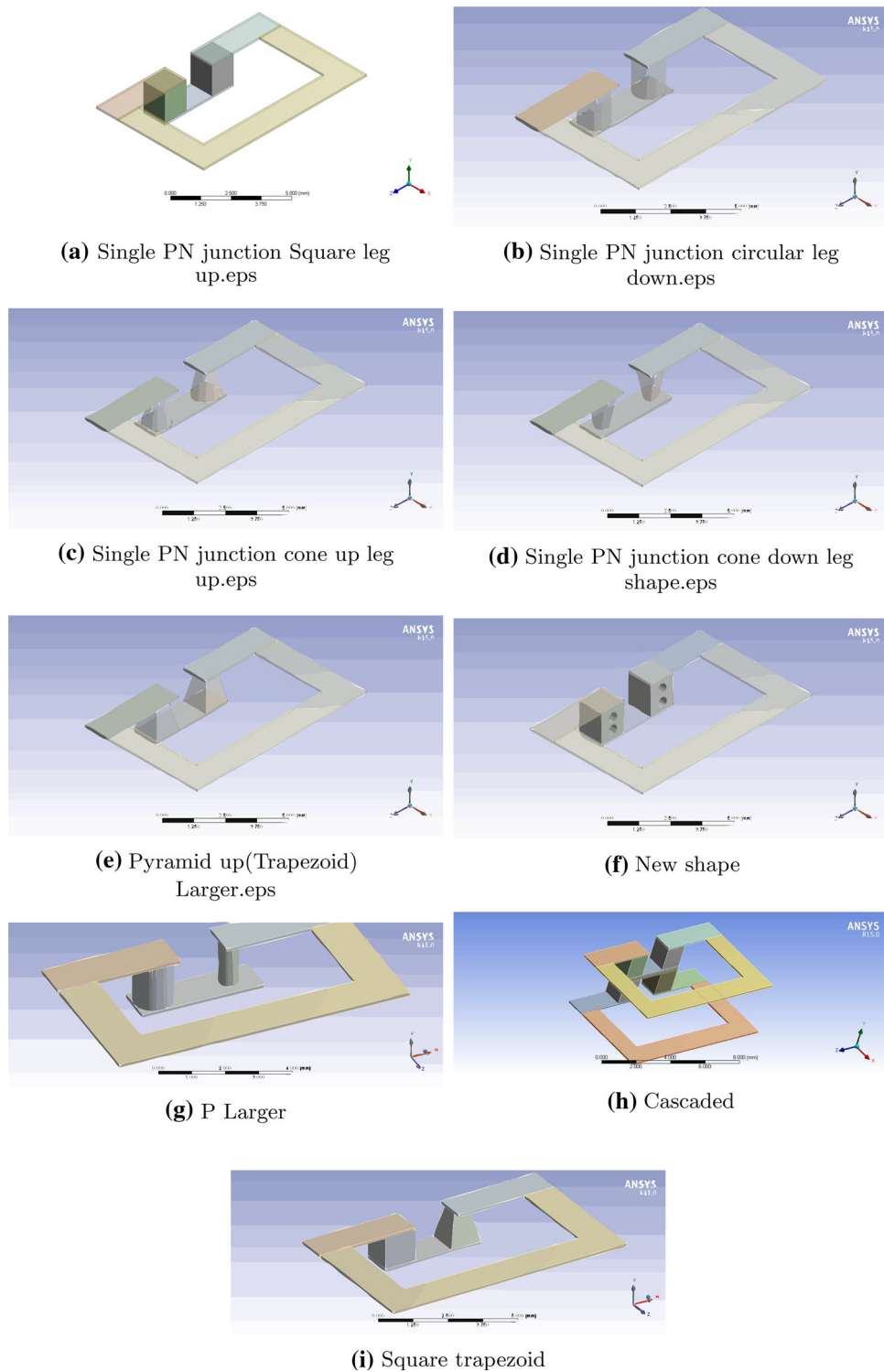
Effect of different geometric shapes on the TEG performance is reported in the next section considering uni-couple.

## 4 Performance analysis of uni-couple thermoelectric generator

A uni-couple TEG consists of one P-type and one N-type semiconductor connected by metals electrode. This section presents the effect of geometric shape, leg length, and cross-sectional area on the performance. The thermal stress developed is also reported in this section.

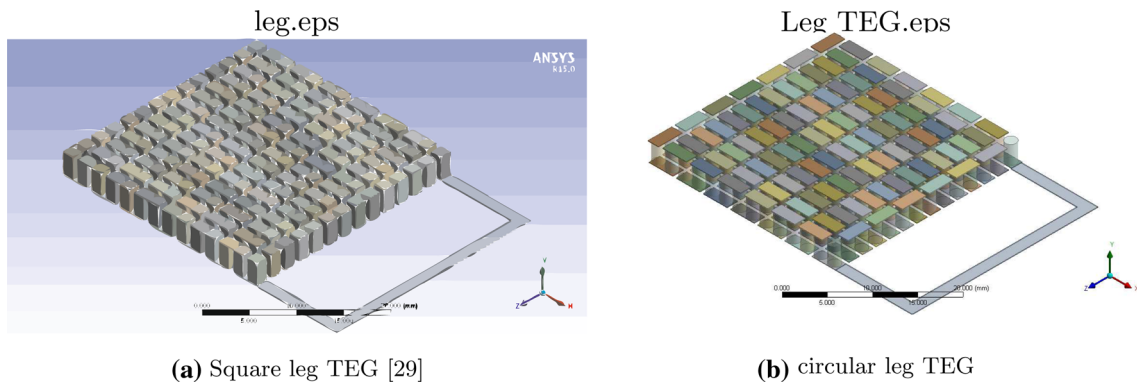
### 4.1 Study of effect of different shapes of TEG

Figure 4 shows different leg shaped TEGs. Simulation is done with hot-side temperature as 700 °C and cold-



**Fig. 4** Different shapes of uni-couple thermoelectric generator





(a) Square leg TEG [29]

(b) circular leg TEG

Fig. 5 TEG of different leg shapes

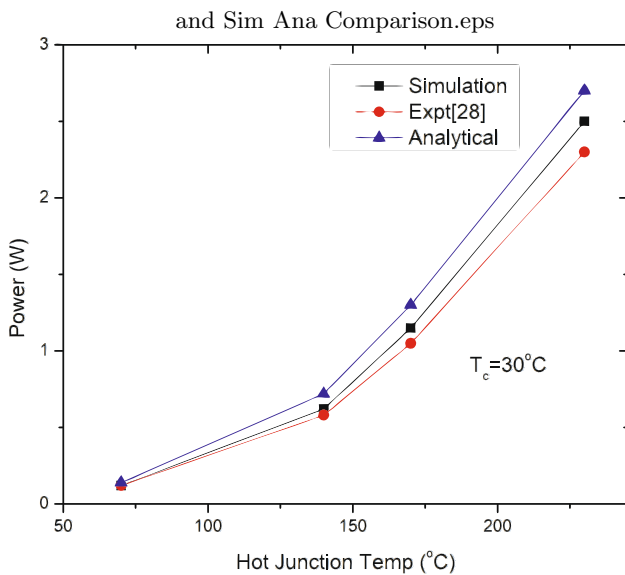
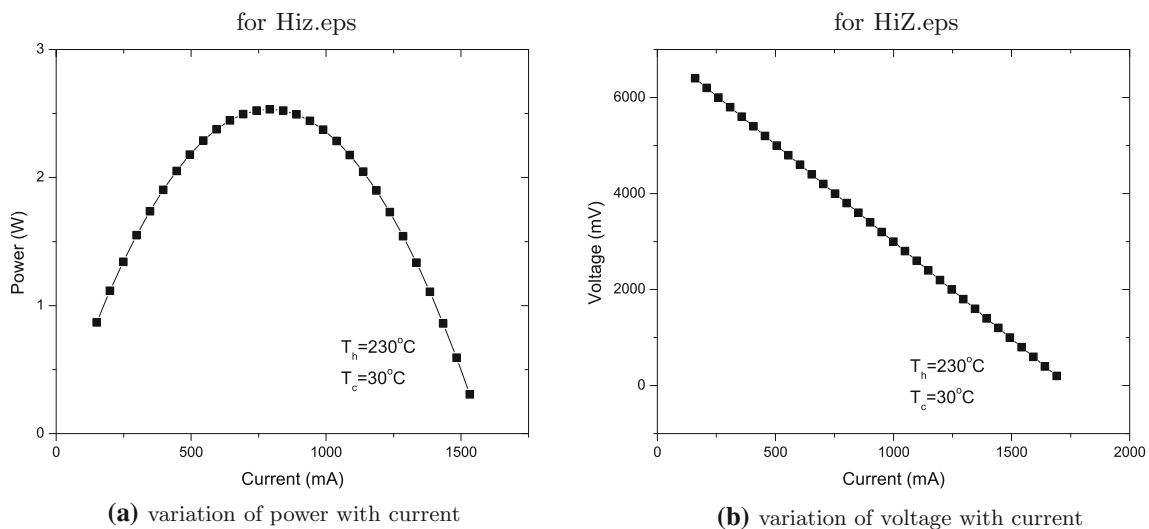


Fig. 6 Variation of power with hot junction temperature

side temperature as  $30^\circ\text{C}$ . The power output of these TEGs with load resistance is shown in Fig. 10. It is observed that for same cross-section area, circular and square leg TEGs have identical power and conversion efficiency but higher compared to other shapes because of Seebeck coefficient; electrical conductivity and thermal conductivity do not depend on shape of leg. The cascaded TEG has the lowest power output. Cascaded or multistage TEG can be used with different material at different stages and can be more efficient.

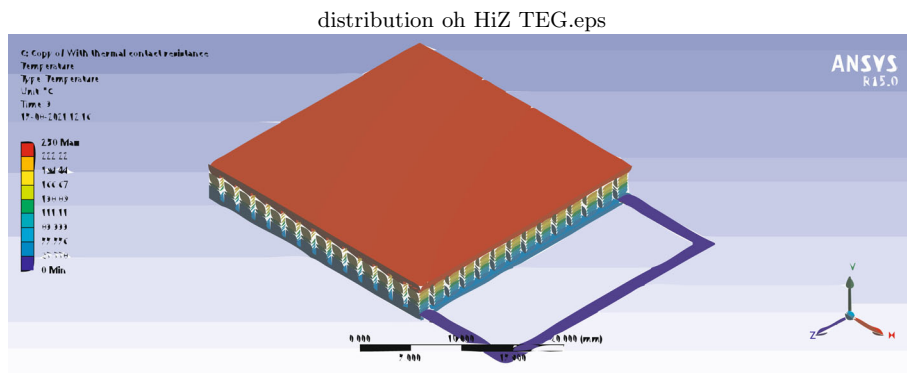
As cross-section area increases more heat enters and it becomes difficult to maintain temperature differences. A new shape shown in Fig. 4f square leg with holes in it which will be effective in maintaining temperature difference. It produces more power than the trapezoid-shaped or cone-shaped leg. Figure 11 shows the efficiency of different TEGs. The trapezoid-shaped TEG is having more conversion efficiency, but power produced is low. Combination of square with trapezoid is producing less power compared to square but more power than trapezoid. The TEG with P-larger has the lowest efficiency at low loads. Power produced by P-type larger TEG is also low.



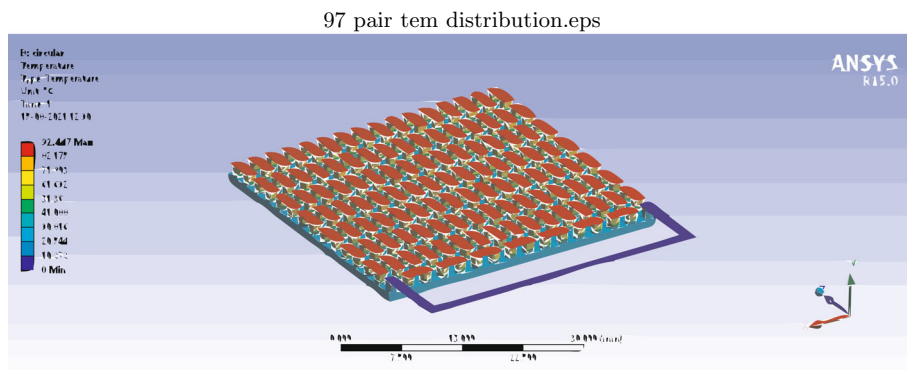
(a) variation of power with current

(b) variation of voltage with current

Fig. 7 Performance analysis of 97 P-N pair TEG(HiZ-2)



(a) Temperature distribution of HiZ-2



(b) circular leg TEG Temperature distribution

Fig. 8 Thermoelectric generator 97 P–N pair

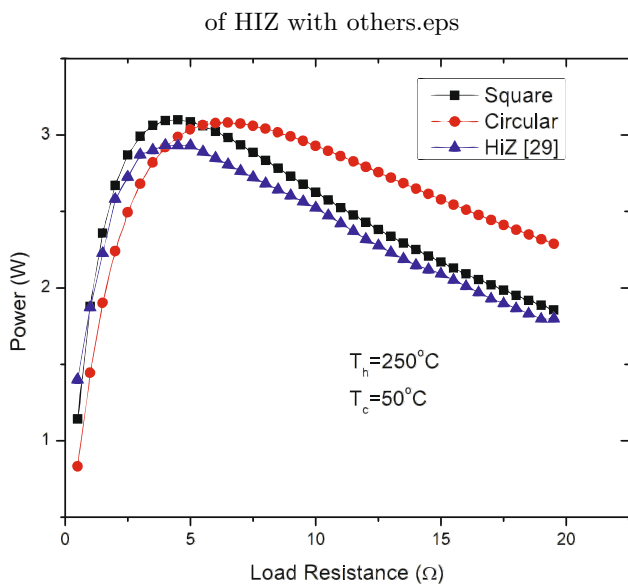


Fig. 9 Effect of load resistance on power

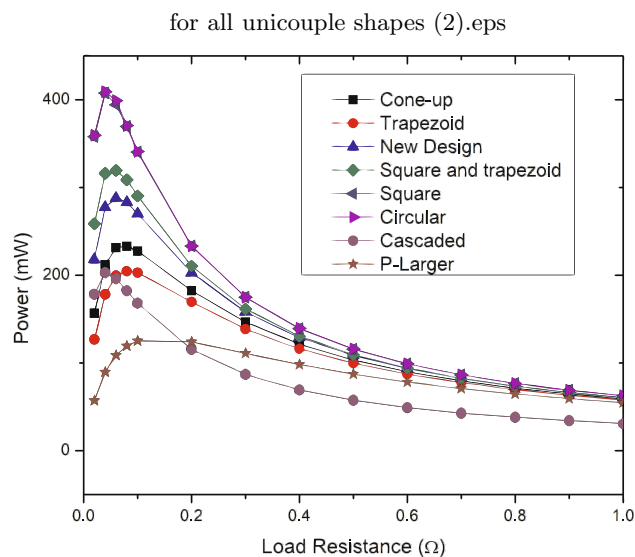


Fig. 10 Effect of load resistance on power for uni-couple TEG

#### 4.1.1 Effect of cross-section area of cone leg

A cone shape TEG is also simulated by keeping base cross-section area same as that of the square leg TEM. The top cross-section area is varied as diameter 0.6 mm and 0.8 mm. It is observed that it produces more power

as the cross-section area increases, as shown in Fig. 12, because more heat flux enters and has more power.

There is not much difference in power produced by cone-up and cone-down the type of thermoelectric module. Even for pyramid-up and down power produced is same as in Fig. 13.

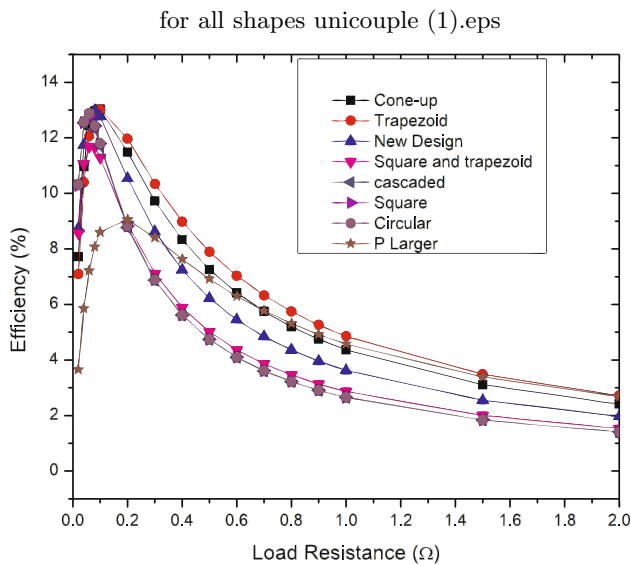


**Fig. 11** Variation of efficiency with load resistance for unicycle TEG

#### 4.1.2 Thermal stress analysis on TEG leg

In a TEG, thermal stresses will develop due to coefficient of thermal expansion as there is temperature difference between the two ends of the generator. It is one of the critical parameters for designing a TEG. The isothermal boundary condition of the hot junction at 500 °C and cold junction at 30 °C is used for simulation. Figure 14a shows max von Mises stress increases as the length of the leg decreases. Figure 14b shows max von Mises stress comparison for various shapes. It can be observed that the pyramid shape has maximum von Mises stress of 794 MPa, square has max von Mises stress of 754 MPa, and circular-shaped leg is having max von Mises stress of 709 Mpa. Figure 14c shows variation of maximum von Mises stress with increase in hot junction temperature and cold junction temperature is at 30 °C. From Fig. 14c, it is observed that maximum von Mises stress increases with an increase in temperature. Figure 14d shows the variation of max von Mises stress with temperature for different leg shapes. Circular-shaped TEG has the lowest stress.

#### 4.1.3 Effect of hot and cold junction temperature

Simulation of TEG is done with the constant temperature difference of 630 °C between hot and cold Junction. The increase the cold junction temperature from 0 to 50 °C decreases the power by 0.75 mw. And increasing the hot junction temperature from 700 to 750 °C decreases the power by 0.58 mw as shown in Fig. 15. Variation in the cold junction temperature has more effect on performance than variation in the hot-side temperature.

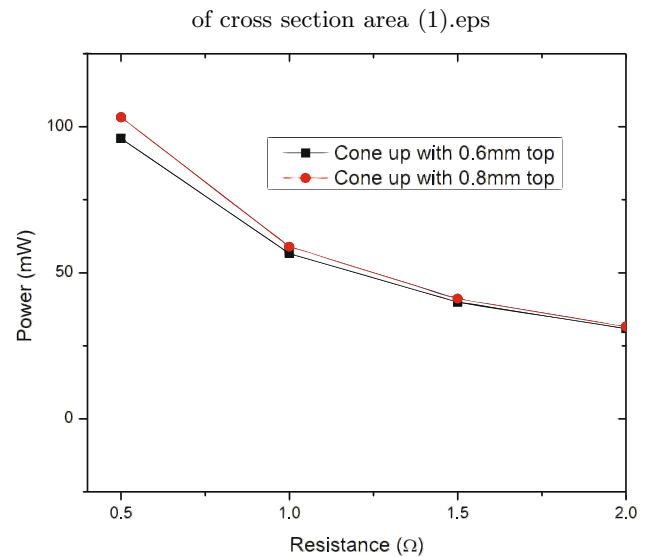


**Fig. 12** Effect of top cross-section area of cone

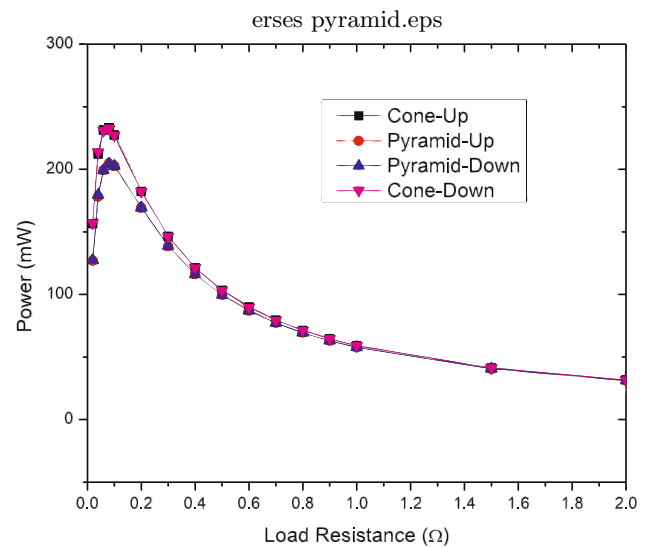


**Fig. 13** Performance analysis of cone, pyramid-up and -down TEG

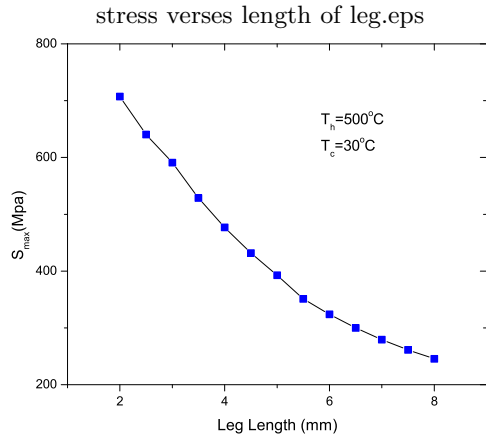
#### 4.1.4 Effect of leg length

Figure 16 shows the effect of leg length on power output. It can be observed that as leg length decreases, power produced increases; however, it is difficult to maintain temperature difference for smaller leg length.

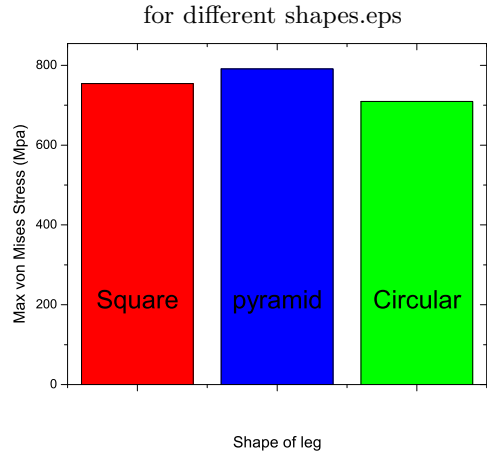
## 5 Conclusions

Performance of thermoelectric generator depends on load resistance and internal resistance. For a particular application, load resistance will be fixed; hence, internal resistance can be changed slightly by varying the geometric parameters. Hence, good performance can be

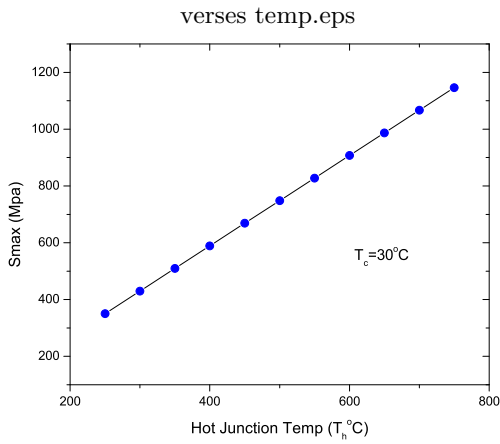




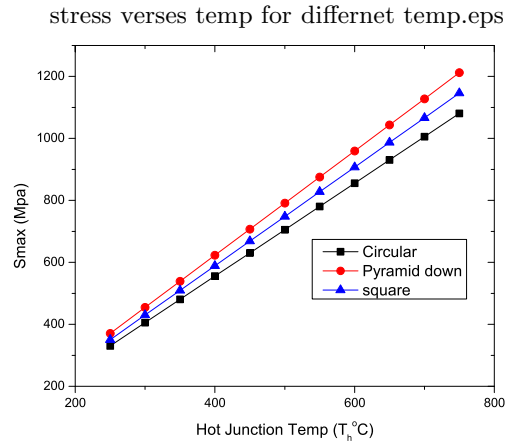
(a) Variation of max von Mises stress with length of leg



(b) Thermal stress for different shapes

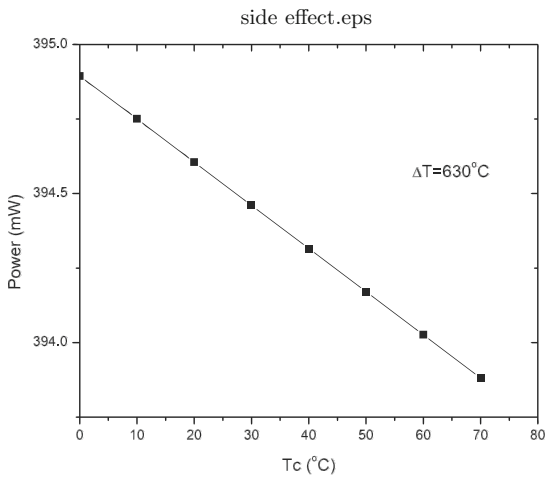


(c) Variation of Max von Mises stress with temperature

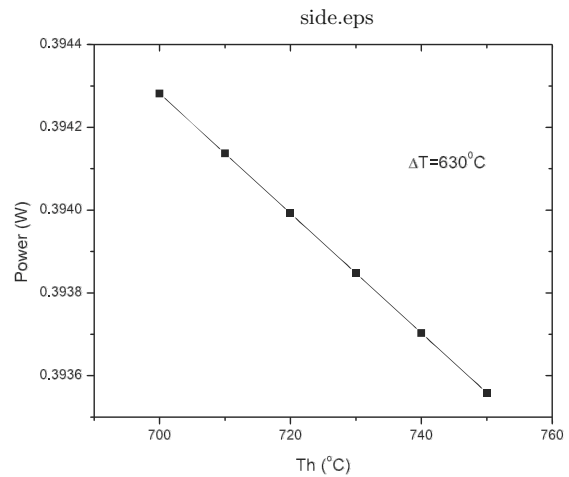


(d) Variation of Max von Mises stress with temperature for different shapes

Fig. 14 Thermal stress analysis



(a) Variation of power with cold junction temperature



(b) Variation of power with hot junction temperature

Fig. 15 Effect of hot and cold junction temperature

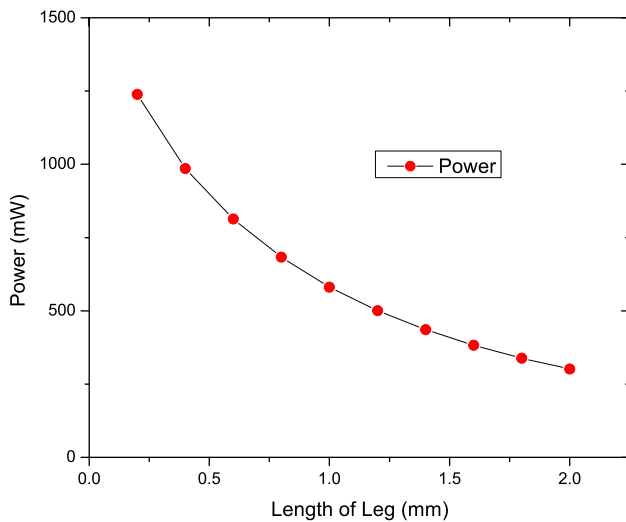


**Fig. 16** Effect of leg length on power

achieved. In this study, the simulated results are compared with experimental results and analytical results for a commercial TEG; all three are good in agreement. The results are also compared with the data sheet provided by the manufacturer. Performance optimization is done for 97 P–N pair thermoelectric generator [Hi-Z2]. The shape of the thermoelectric generator's leg is varied from square- to circular-shaped leg. It is observed that at low load resistance, square-shaped TEG is good, but for larger load resistance, circular TEG is better.

Different shapes of uni-couple thermoelectric generators are analysed, and it is observed that with same cross-section area, square and circular leg TEG produces identical power and efficiency whereas, circular leg TEG will have lower thermal stress. Trapezoid shaped leg is having higher efficiency compared to other shapes. Variation in the cold junction temperature has a higher effect on performance than variation in the hot-side temperature.

**Acknowledgements** The author acknowledges Prof. Ramesh Chandra Mallik, Indian Institute of Science Bangalore for fruitful discussion and support. Authors acknowledges Vision Group on Science and Technology (VGST) (Grant No. KSTePS/VGST-K-FIST L2/2078-L9 / GRD No.765).

## References

1. P. Malaji, S. Ali, S. Adhikari, M. Friswell, Analysis of harvesting energy from mistuned multiple harvesters with and without coupling. *Procedia Eng.* **144**, 1065–1073 (2016)
2. P. V. Malaji, Analysis of pendulum-based nonlinear energy sink for energy harvesting. In: *Trends in Manufacturing and Engineering Management. Lecture Notes*

*in Mechanical Engineering*, pp. 467–478, Springer, (2021)

3. M. Alhawari, B. Mohammad, H. Saleh, M. Ismail, A survey of thermal energy harvesting techniques and interface circuitry. In: *2013 IEEE 20th International Conference on Electronics, Circuits, and Systems (ICECS)*, pp. 381–384, IEEE, (2013)
4. X. Lu, S.-H. Yang, Thermal energy harvesting for WSNS. In: *2010 IEEE International Conference on Systems, Man and Cybernetics*, pp. 3045–3052, IEEE, (2010)
5. D. Champier, Thermoelectric generators: a review of applications. *Energy Convers. Manage.* **140**, 167–181 (2017)
6. D. Ebling, A. Krumm, B. Pfeiffelmann, J. Gottschald, J. Bruchmann, A.C. Benim, M. Adam, R. Herbertz, A. Stunz et al., Development of a system for thermoelectric heat recovery from stationary industrial processes. *J. Electron. Mater.* **45**(7), 3433–3439 (2016)
7. J. Caban, Technologies of using energy harvesting systems in motor vehicles—energy from exhaust system
8. Q. Zhang, J. Liao, Y. Tang, M. Gu, C. Ming, P. Qiu, S. Bai, X. Shi, C. Uher, L. Chen, Realizing a thermoelectric conversion efficiency of % in bismuth telluride/skutterudite segmented modules through full-parameter optimization and energy-loss minimized integration. *Energy Environ. Sci.* **10**(4), 956–963 (2017)
9. C. Wang, S. Tang, X. Liu, G. Su, W. Tian, S. Qiu, Experimental study on heat pipe thermoelectric generator for industrial high temperature waste heat recovery. *Appl. Therm. Eng.* **175**, 115299 (2020)
10. D. Rowe, General principles and basic considerations. In: *Thermoelectrics Handbook*, pp. 26–40, CRC press, (2018)
11. G. J. Snyder, E. S. Toberer, Complex thermoelectric materials. In: *Materials for Sustainable Energy: A Collection of Peer-Reviewed Research and Review Articles from Nature Publishing Group*, pp. 101–110, (2011)
12. R. Kondaguli, P. Malaji, Mathematical modeling and numerical simulation of thermoelectric generator. *AIP Conf. Proc.* **2274**, 030037 (2020). (AIP Publishing LLC)
13. L.-D. Zhao, S.-H. Lo, Y. Zhang, H. Sun, G. Tan, C. Uher, C. Wolverton, V.P. Dravid, M.G. Kanatzidis, Ultralow thermal conductivity and high thermoelectric figure of merit in SNSE crystals. *Nature* **508**(7496), 373–377 (2014)
14. P.-P. Shang, J. Dong, J. Pei, F.-H. Sun, Y. Pan, H. Tang, B.-P. Zhang, L.-D. Zhao, J.-F. Li, Highly textured N-type SNSE polycrystals with enhanced thermoelectric performance. *Research*, **2019**, (2019)
15. C.B. Vining, An inconvenient truth about thermoelectrics. *Nat. Mater.* **8**(2), 83–85 (2009)
16. P. Ziolkowski, P. Blaschkewitz, E. Müller, Heat flow measurement as a key to standardization of thermoelectric generator module metrology: a comparison of reference and absolute techniques. *Measurement* **167**, 108273 (2021)
17. H. Lee, J. Sharp, D. Stokes, M. Pearson, S. Priya, Modeling and analysis of the effect of thermal losses on thermoelectric generator performance using effective properties. *Appl. Energy* **211**, 987–996 (2018)

18. A. Elarusi, N. Illendula, H. Fagehi, Performance prediction of commercial thermoelectric generator modules using the effective material properties. *Western Michigan University*, (2014)
19. Z. Luo, A simple method to estimate the physical characteristics of a thermoelectric cooler from vendor datasheets. *Electron. Cool.* **14**(3), 22–27 (2008)
20. S. Lineykin, S. Ben-Yaakov, Modeling and analysis of thermoelectric modules. *IEEE Trans. Ind. Appl.* **43**(2), 505–5 (2007)
21. D.R. Karana, R.R. Sahoo, Influence of geometric parameter on the performance of a new asymmetrical and segmented thermoelectric generator. *Energy* **179**, 90–99 (2019)
22. G. Min, D. Rowe, Optimisation of thermoelectric module geometry for ‘waste heat’electric power generation. *J. Power Sources* **38**(3), 253–259 (1992)
23. S. Kumar, S.D. Heister, X. Xu, J.R. Salvador, Optimization of thermoelectric components for automobile waste heat recovery systems. *J. Electron. Mater.* **44**(10), 3627–3636 (2015)
24. H. Ali, A.Z. Sahin, B.S. Yilbas, Thermodynamic analysis of a thermoelectric power generator in relation to geometric configuration device pins. *Energy Convers. Manage.* **78**, 634–640 (2014)
25. L. Fan, G. Zhang, R. Wang, K. Jiao, A comprehensive and time-efficient model for determination of thermoelectric generator length and cross-section area. *Energy Convers. Manage.* **122**, 85–94 (2016)
26. H. He, Y. Wu, W. Liu, M. Rong, Z. Fang, X. Tang, Comprehensive modeling for geometric optimization of a thermoelectric generator module. *Energy Convers. Manage.* **183**, 645–659 (2019)
27. A. Fabián-Mijangos, G. Min, J. Alvarez-Quintana, Enhanced performance thermoelectric module having asymmetrical legs. *Energy Convers. Manage.* **148**, 1372–1381 (2017)
28. S. Weera, H. Lee, A. Attar, Utilizing effective material properties to validate the performance of thermoelectric cooler and generator modules. *Energy Convers. Manage.* **205**, 1427 (2020)
29. H.-Z. manufacturer, Hiz data sheet. *Hi Z* **1**(1), 1 (2019)
30. R. Kondaguli, P. Malaji, Analysis of bismuth telluride (bi<sub>2</sub>te<sub>3</sub>) thermoelectric generator. In *2020 IEEE Bangalore Humanitarian Technology Conference (B-HTC)*, pp. 1–5, IEEE, (2020)
31. E. E. Antonova, D. C. Looman, Finite elements for thermoelectric device analysis in ansys. In: *ICT 2005. 24th International Conference on Thermoelectrics, 2005.*, pp. 215–218, IEEE, (2005)
32. A.F. Ioffe, L. Stil’Bans, E. Iordanishvili, T. Stavitskaya, A. Gelbtuch, G. Vineyard, Semiconductor thermoelements and thermoelectric cooling. *Phys. Today* **12**(5), 42 (1959)
33. P. Ponnusamy, J. de Boor, E. Müller, Using the constant properties model for accurate performance estimation of thermoelectric generator elements. *Appl. Energy* **262**, 114587 (2020)
34. R. Courant, Variational methods for the solution of problems of equilibrium and vibrations. *Bull. Am. Math. Soc.* **49**(1), 1–23 (1943)
35. P. G. Lau, R. J. Buist, Temperature and time dependent finite-element model of a thermoelectric couple. In: *Fifteenth International Conference on Thermoelectrics. Proceedings ICT’96*, pp. 227–233, IEEE, (1996)